High temperatures augment inhibition of parasites by a honey bee gut symbiont

Running title: Temperature-dependent inhibition of bee parasites

Evan C Palmer-Young [1]*, Lindsey M Markowitz [1,2], Wei-Fone Huang [1], Jay D Evans [1]

[1] USDA-ARS Bee Research Lab, Beltsville, MD, USA

[2] Department of Biology, University of Maryland, College Park, MD, USA

*Corresponding author: ecp52@cornell.edu, evan.palmer-young@usda.gov

ABSTRACT

Temperature affects growth, metabolism, and interspecific interactions in microbial communities. Within animal hosts, gut bacterial symbionts can provide resistance to parasitic infections. Infection can also be shaped by host body temperature. However, the effects of temperature on the antiparasitic activities of gut symbionts have seldom been explored. The *Lactobacillus*-rich gut microbiota of facultatively endothermic honey bees is subject to seasonal and ontogenetic changes in host temperature that could alter the effects of symbionts against parasites. We used cell cultures of a *Lactobacillus* symbiont and an important trypanosomatid gut parasite of honey bees to test the potential for temperature to shape parasite-symbiont interactions.

We found that symbionts showed greater heat tolerance than parasites and chemically inhibited parasite growth via production of acids. Acceleration of symbiont growth and acid production at high temperatures resulted in progressively stronger antiparasitic effects across a temperature range typical of bee colonies. Consequently, the presence of symbionts reduced both peak growth rate and heat tolerance of parasites. Results suggest that the endothermic behavior of honey bees could potentiate the effectiveness of gut symbionts that limit parasites' ability to withstand high temperature, implicating thermoregulation as a reinforcer of core symbioses and possibly microbiome-mediated antiparasitic defense.

IMPORTANCE

Two factors that shape the resistance of animals to infection are body temperature and gut microbiota. However, temperature can also alter interactions among microbes, raising the question of whether and how temperature changes the antiparasitic effects of gut microbiota. Honey bees are agriculturally important hosts of diverse parasites and infection-mitigating gut microbes. They can also socially regulate their body temperatures to an extent unusual for an insect. We show that high temperatures found in honey bee colonies augment the ability of a gut bacterial symbiont to inhibit growth of a common bee parasite and reduce the parasite's ability to grow at high temperatures. This suggests that fluctuations in colony and body temperatures across life stages and seasons could alter the protective value of bees' gut microbiota against parasites, and that temperature-driven changes in gut microbiota could be an underappreciated mechanism by which temperature— including endothermy and fever— alters animal infection.

Keywords: thermal performance curve, metabolic theory of ecology, microbiome, infectious disease ecology, thermoregulation

INTRODUCTION

Temperature has a fundamental effect on biological rates that influence organismal physiology and interspecific interactions (1–4), including infection of hosts by parasites (5–8). The influence of temperature on infection outcome reflects not merely the direct effects of temperature on the performance of parasites, but on parasites' performance relative to that of the host and its immune system (6, 8). In many hosts, attainment of high internal temperatures can reduce the intensity and effects of infection (9–13), whether due to direct inactivation of parasites or potentiation of host immunity (10, 14–16). Such temperature-mediated increases in host resistance to infectious disease could favor the evolution of energetically expensive, endothermic life history strategies characterized by sustained high body temperatures (17).

In addition to the defenses of the host itself, parasites that establish in the gut are also influenced by cooccurring species that form the host gut microbiota and are likewise influenced by host temperature. The community of non-pathogenic microbial species (hereafter referred to as 'symbionts', although this term *sensu stricto* includes all host-associated species) in the host gut can substantially influence infection outcome via physical, chemical, and host immune system-mediated effects (18). A growing number of studies have indicated that temperature influences the composition of the gut symbiont community in ways that are qualitatively similar across distantly related hosts (19). However, despite the known effects of temperature on microbial community composition, biochemistry, and the microbiome and parasitic infection of hosts, the ways in which temperature alters the effects of gut symbionts on parasites has received little attention (19). A more complete knowledge of this area would elucidate how climate and host thermoregulation, including the constitutively high body temperatures of endotherms and infection-associated elevations in body temperature known as 'fever', could affect parasitism via symbiont-driven effects.

Honey bees and their associated microbiota offer an excellent opportunity to study the joint effects of temperature and gut symbionts on parasites. Honey bees are facultatively endothermic, capable of sustaining body and hive temperatures that are similar to those of mammals . Like other insects, however, they are subject to wide temperature variations during outdoor foraging and in the winter (20, 21). Honey bees also possess a broadly consistent, culturable gut bacterial community (22, 23) that can improve host resistance to parasites (24) that can threaten colony health (25–27).

Trypanosomatid parasites of the honey bee hindgut, namely *Crithidia mellificae* (28) and the currently dominant *Lotmaria passim* (29), are prevalent, widespread, and in some cases associated with shortened bee lifespan and colony losses (26, 30–36). These honey bee-associated species are close relatives of the bumble bee parasite *Crithidia bombi. Crithidia bombi* infection is profoundly affected by the bumble bee gut microbiota (37, 38), which is taxonomically similar to that of honey bees (39). This includes negative correlations with the abundance of *Lactobacillus* 'Firm-5' clade members (38, 40), which colonize the hindgut of honey bees as well (39, 41–43). Bumble bee-associated *Lactobacillus* symbionts exerted temperature-dependent, acidity-driven effects on *C. bombi* growth in cell cultures (44, 45), and could contribute to the reduction of infection seen in bees reared at high temperatures (37 °C (46)). The gut microbiota of other insects can also influence infection with trypanosomatids, including species of medical and veterinary importance (47). However, the effects of the honey bee microbiome, including Lactobacilli, on trypanosomatid infection remain unclear. The only work thus far that tested the effects of gut microbial manipulations on infection found that pre-treatment of worker bees with another symbiont, *Snodgrassella alvi,* resulted in greater intensities of *L. passim* infection (48).

To evaluate how temperature affects growth rates of honey bee *Lactobacillus* symbionts relative to trypanosomatid parasites and the effects of symbionts on parasite growth, we conducted three sets of experiments to: (1) Compare the temperature dependence of parasite and symbiont growth rates; (2)

test for effects of symbionts and the acids they produce on parasite growth; and (3) determine how the effects of symbionts vary with temperature and alter the thermal niche of parasites. Our results show that the high colony temperatures produced by the endothermic behavior of bees can selectively favor the growth of symbionts and their inhibition of parasites, such that the presence of symbionts effectively reduces parasite heat tolerance.

MATERIALS AND METHODS

Cell Cultures

Two strains of *Lactobacillus* nr. *melliventris* (49), kindly provided by N.J. Moran and J.E. Powell, were grown in De Man, Rogosa and Sharpe (MRS) media supplemented with 0.05% cysteine in screw-cap microcentrifuge tubes at 37 °C. These isolates are hereafter referred to by full genus and strain names, for consistency with their original description and to differentiate their genus from *Lotmaria.* The honey bee trypanosomatid parasites *C. mellificae* (ATCC 30254 (28)) and *L. passim* (strain BRL (29)) were obtained from the American Type Culture Collection and R.S. Schwarz. Trypanosomatids were grown in “FPFB” medium including 10% heat-inactivated fetal bovine serum (pH 5.9-6.0 (50)) at 28 °C in vented cell culture flasks. Cultures were transferred to fresh media every 2 d.

Effects of temperature on symbiont vs. parasite growth rate

Dense cultures (net OD ~0.8) were diluted to a starting OD of 0.010 in fresh media and incubated in microcentrifuge tubes at 3 °C increments between 25 and 46 °C. We ran six experimental blocks, each of which used parallel incubations at 7 different temperatures (3 blocks in 3 °C increments from 25-43 °C and 3 blocks from 28-46 °C). One replicate tube per strain and temperature was destructively sampled at each of two time points (18 and 24 h). Growth rates were calculated as the

slope of the curve of ln(OD) vs. time using the 18 h time point only, at which point we could be confident that cultures were still in the logarithmic phase of growth. For comparison, we used previously reported growth rates of the two honey bee trypanosomatids (51), which included two replicate runs per temperature at 20 °C and in 2 °C increments from 23-41 °C, plus a third replicate for each of four temperatures (25, 31, 33, and 35 °C).

We modeled the temperature dependence of growth rate for each *Lactobacillus* and trypanosomatid strain using a Sharpe-Schoolfield equation modified for high temperatures (15, 52, 53).

$$rate(T) = \frac{r_{T_{ref}} \cdot e^{\frac{-E}{k}\left(\frac{1}{T} - \frac{1}{T_{ref}}\right)}}{1 + e^{\frac{E_h}{k}\left(\frac{1}{T_h} - \frac{1}{T}\right)}} \quad (1)$$

In Equation (1), *rate* refers to the maximum specific growth rate (in [h^{-1}]); r_{Tref} is the growth rate (in [h^{-1}]) at the calibration temperature T_{ref} (293K, i.e., 20°C, chosen to be well below the temperature of peak rate)); E is the activation energy (in eV), which primarily affects the upward-sloping portion of the thermal performance curve (i.e., responsiveness of growth to temperature) at suboptimal temperatures; k is Boltzmann's constant ($8.62 \cdot 10^{-5}$ eV·K^{-1}); E_h is the deactivation energy (in eV), which determines how rapidly the thermal performance curve decreases at temperatures above the temperature of peak growth T_{pk} (in K); T_h is the high temperature (in K) at which growth rate is reduced by 50% (relative to the value predicted by the Arrhenius equation—which assumes a monotonic, temperature-dependent increase) (53); and T is the experimental incubation temperature (in K). Four models were fit, one for each strain of *Lactobacillus* and each trypanosomatid (51).

Models were optimized using nonlinear least squares, implemented with R packages rTPC and nls.multstart (54). Confidence intervals on parameter values and predicted growth rates were obtained by bootstrap resampling of the residuals (10,000 model iterations, R package "car" (55)). Expected ratios

between growth rates of symbionts and parasites were calculated by dividing the average of the predicted growth rates for the two *Lactobacillus* strains by the predicted rates for each of the trypanosomatid species at the corresponding temperature. We also used the bootstrap model predictions to estimate the following traits not explicitly included in the model: peak growth rate; temperatures of peak growth rate (T_{pk}), and 50% inhibition relative to the peak value due to low and high temperatures (referred to as "cold tolerance" and "heat tolerance" in figures); and thermal niche breadth (i.e., the number of degrees between the low and high temperatures of 50% rate inhibition). The 0.025 and 0.975 quantiles for parameter estimates, predicted growth rates at each temperature, and traits derived from bootstrap predictions were used to define 95% confidence intervals. Estimates from different models were considered significantly different from each other when their 95% confidence intervals did not overlap. This and all subsequent analyses were conducted using R for Windows v4.0.3 (56).

Effects of symbiont spent medium and acidity on parasite growth

To generate spent media, each of the two *Lactobacillus* strains was grown in 15 mL conical centrifuge tubes for 2 d at 37 °C from a 100x dilution of stationary phase cultures. The resulting supernatant (pH 4.6) was sterile-filtered, and an aliquot was neutralized with 1M NaOH to the original pH of the MRS media (pH 5.6). Meanwhile, an aliquot of fresh MRS media was acidified with glacial acetic acid (the main acid in the honey bee gut (57) and of isolated *Lactobacillus melliventris* under aerobic conditions (57)) to the pH of the spent media (pH 4.6). Each of the two trypanosomatids was then grown in a mixed growth medium consisting of equal volumes of fresh trypanosomatid-specific "FPFB" media and one of six *Lactobacillus*-specific MRS media-based treatments: spent or neutralized media from each of the two *Lactobacillus* strains, acidified MRS media, or a fresh MRS media control.

The spent media treatments tested for symbiont-mediated inhibition of parasite growth; the acidified fresh media and neutralized spent media treatments indicated the extent to which this inhibition was dependent on pH.

To assess parasite growth, cell cultures of each trypanosomatid were diluted to a net OD of 0.040 in the appropriate mixed media. Growth of n = 6 replicate wells per treatment was measured in 96-well plates incubated in a plate reader spectrophotometer at 31 °C. We included cell-free negative controls for each of the MRS media treatments, to control for changes in OD of media independent of parasite growth. OD values were corrected by subtraction of the OD of the corresponding cell-free media treatment and time point. Growth was estimated by measurement of optical density (OD) at 600 nm in 5 min intervals for 24 h, with a 30 s shake before each read. Growth rate was calculated as the maximum slope of ln(OD) vs. time over a rolling 4 h window, after exclusion of the first 3 h to allow OD to stabilize (15, 51, 58). Samples for which the r-squared value for the growth rate fell below 0.9 (vs. >0.98 for all non-acidified samples) were considered to have a negligible growth rate and were assigned a rate of 0. Visual inspection of growth curves indicated that none of these samples exceeded a net OD of 0.050.

Temperature-dependent effects of symbionts on parasite growth in parasite-symbiont cocultures

To evaluate how temperature modulates the ability of symbionts to inhibit parasites, we grew *L. passim* in the presence and absence of *Lactobacillus* strain wkB10 at temperatures between 20.7 and 38 °C, which spans the range of temperatures commonly observed in worker bees within the winter cluster of colonies in a temperate climate (21). A dense culture of *L. passim*, grown 2 d at 28 °C from a 25-fold

dilution, was diluted to a net OD of 0.020 in fresh FPFB media. A dense culture of *Lactobacillus* strain wkB10, grown 2 d at 37 °C from a 100-fold dilution, was diluted to a net OD of 0.040 in fresh MRS media. The *L. passim* cell suspension was then mixed with an equal volume of either the *Lactobacillus* cell suspension ("*Lactobacillus* present" treatment, initial net OD of 0.010 for the parasite and 0.020 for the symbiont) or fresh MRS without cells ("*Lactobacillus* absent"). These initial densities were chosen such that *L. passim* would remain in log-phase growth throughout the experiment, while *Lactobacillus* would approach stationary phase at the higher temperatures.

Two replicate microcentrifuge tubes, each containing 1400 µL of media, were incubated in parallel for 23 h at each of 7 different temperatures; two additional tubes were refrigerated at ~0 °C immediately following setup for measurement of initial cell densities and media pH. Following the incubation, parasite densities were quantified by microscopic cell counts using a Neubauer hemocytometer at 400x magnification, using a 100 µL aliquot of each tube diluted with an equal volume of 50% glycerol to slow the movement of the parasite cells. Parasite growth rates were estimated based on the ratio of parasite cell densities at 23 h vs 0 h of incubation. The remaining sample volume was used for measurement of pH. The experiment was repeated 3 times for a total of 6 replicate samples per temperature and *Lactobacillus* treatment.

To quantify the temperature dependence of parasite growth rate, separate Sharpe-Schoolfield models were fit to the data for parasite growth rate in the presence and absence of *Lactobacillus*, using the approach described above (Methods: Effects of temperature on symbiont vs. parasite growth rate). To compute the proportion of parasite growth inhibition by *Lactobacillus*, we averaged growth rates of the two *Lactobacillus*-containing and *Lactobacillus*-free replicates within each temperature and experimental block. Percent inhibition was then computed from the ratios of growth rates in the presence vs. absence of *Lactobacillus* for each temperature-block combination.

We modeled the correlations between temperature and parasite inhibition, temperature and pH, and pH and parasite inhibition using generalized linear models (59). Each model included experiment block as a random effect. In addition, the models for the effects of temperature and of pH on parasite inhibition included quadratic predictor terms (i.e., $(\text{temperature})^2$, $(\text{pH})^2$) to better describe the curvilinear relationship between these variables that was apparent from visual inspection of the data. Models were fit using R package glmmTMB (59), with predictions generated with R package emmeans (60). Graphs were produced using R packages ggplot2 and cowplot (61, 62).

RESULTS

Effects of temperature on growth rates. Relative to the trypanosomatid parasites measured in our previous experiments (51)), growth of both strains of *Lactobacillus* symbionts increased more strongly with temperature and peaked at higher temperatures, resulting in progressively higher projected growth rates of the symbionts relative to the parasites--particularly *L. passim*—as temperatures increased **(Figure 1).** *Lactobacillus* growth rates increased by 6- to 7-fold over the 15 °C temperature window between 25 and 40 °C, whereas growth rates of trypanosomatids varied by <2-fold over a similar 15 °C interval from 20 to 35 °C. These differences in temperature responsiveness were reflected in the estimates for activation energy (model parameter *E*), which was more than twice as high in both strains of *Lactobacillus t*han in either species of trypanosomatid (**Figure 2; see Supplementary Figure 1** for additional parameters). In addition, *Lactobacillus g*rowth rates peaked at temperatures more than 4 °C higher than those of *C. mellificae* and more than 6 °C higher than those of *L. passim* **(Figure 2)**. The more steeply angled, high temperature-shifted thermal performance curves of the two Lactobacilli were likewise reflected by their higher temperatures of cold- and heat-related 50% growth

inhibition and narrower thermal breadth (i.e., width of the thermal interval over which growth rates exceeded 50% of the peak value**,** **Supplementary Figure 2**).

Based on model predictions, the expected growth rates of symbionts relative to trypanosomatids increased with temperature across the 25-37 °C interval that is most common in honey bee workers (21), changing by 4.67-fold for *Lactobacillus* (averaged across the two strains) relative to *C. mellificae* and 9.25-fold relative to *L. passim* **(Figure 1).** Even over the narrow 33.8-37 °C temperature range of the central honey bee brood cluster (20), growth rates of *Lactobacillus* increased by 65% relative to *C. mellificae* and by more than 3-fold relative to *L. passim* (**Figure 1**).

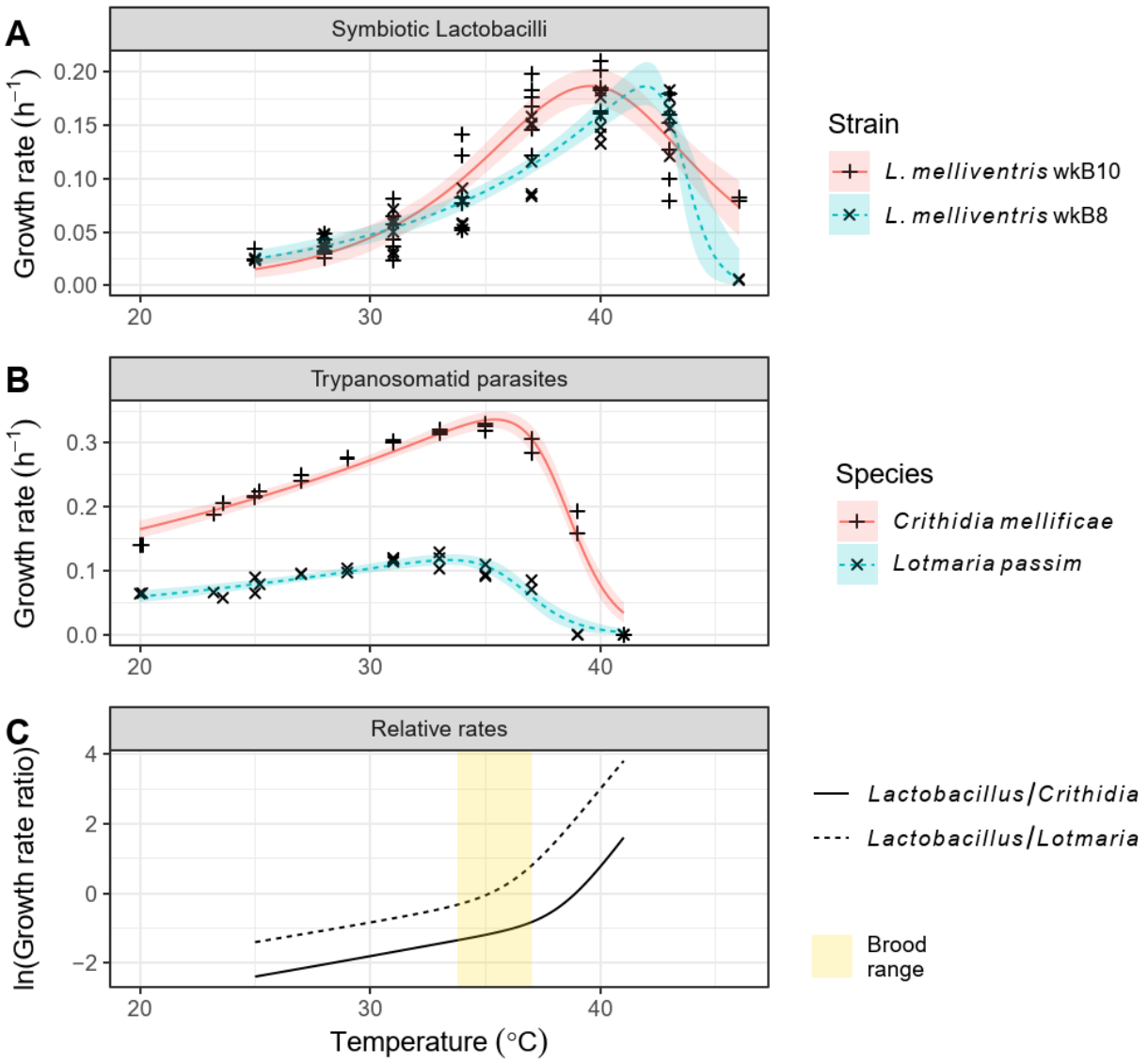

239

240 **Figure 1. Growth of *Lactobacillus melliventris* honey bee gut symbionts responds more strongly to**

241 **temperature and persists at higher temperatures than growth of the trypanosomatid parasites**

242 ***Crithidia mellificae* and *Lotmaria passim*. (A)** Growth rates of *Lactobacillus* strains wkB8 (solid lines) and

243 wkB10 (dashed lines) between 25 and 46 °C. Points show observed rates. Lines and shaded bands show

244 Sharpe-Schoolfield model predictions and 95% bootstrap confidence intervals. **(B)** Sharpe-Schoolfield

245 models for temperature-dependent growth of *C. mellificae* (solid lines) and *L. passim* (dashed lines), as

246 reported previously (51). **(C)** Projected growth rates of *Lactobacillus* (average of strains wkB8 and

247 wkB10) relative to *C. mellificae* (solid lines) and *L. passim* (dashed lines) between 25 and 41 °C. Yellow

248 shaded region represents temperature range at center of brood-rearing honey bee colony (33.8-37 °C
249 (20)).

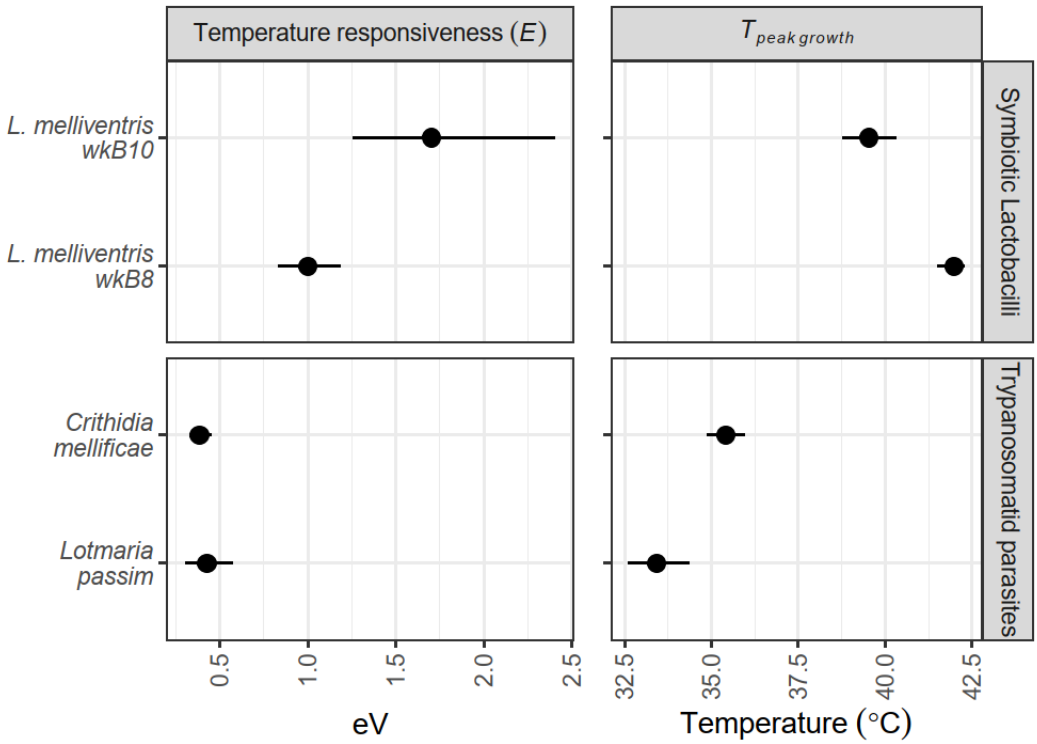

250

251 **Figure 2. Growth rates of symbiotic Lactobacilli (upper panels) were more responsive to temperature**
252 **and peaked at higher temperatures than did growth of trypanosomatid gut parasites (lower panels).**
253 Left panels show Sharpe-Schoolfield model parameter *E*, a measure of how strongly growth rate
254 increases with temperature at temperatures below the temperature of peak growth (right panels).
255 Points and error bars show bootstrap medians and 95% confidence intervals.

256

257 **Acidity-mediated inhibitory effects of *Lactobacillus* spent media.** Spent media from each of the
258 two *Lactobacillus* strains resulted in full inhibition of both *C. mellificae* and *L. passim* (**Figure 3**).
259 Acidification of fresh media to an equivalent pH with acetic acid likewise extinguished growth, whereas

neutralization of the spent media restored 89-90% of growth in *C. mellificae* and 81-82% in *L. passim,* indicating that acidity was necessary and sufficient to account for most of the observed inhibition by spent media (**Figure 3**).

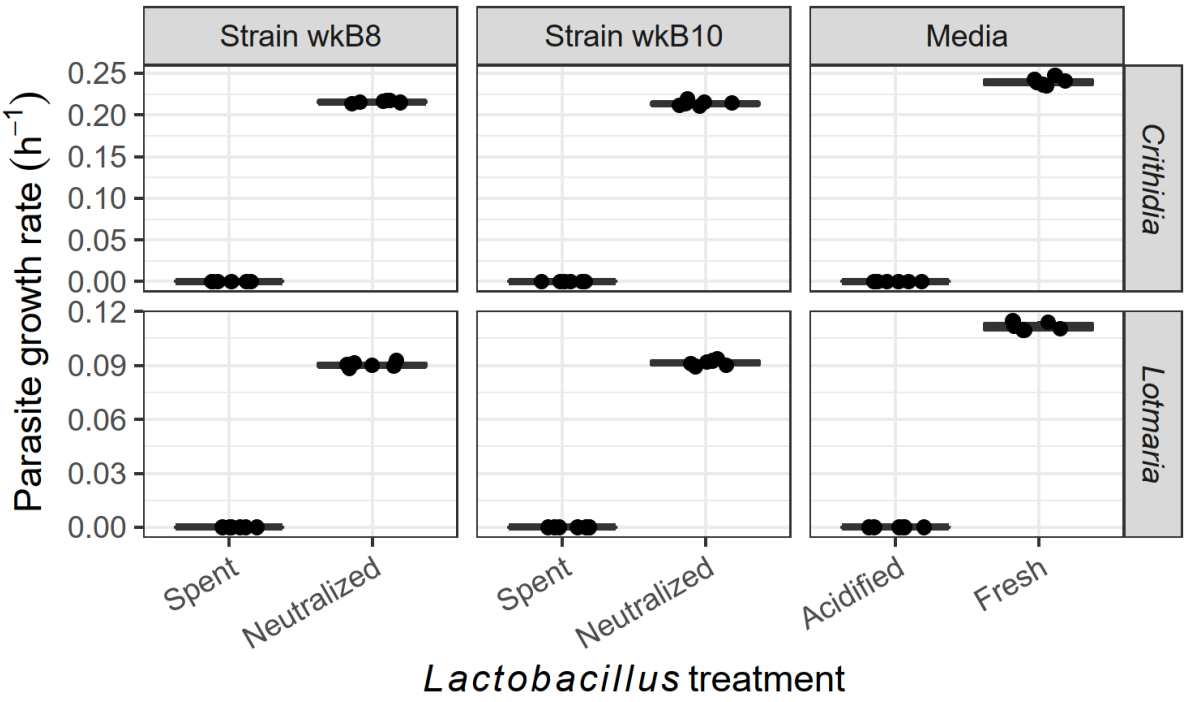

Figure 3. Acidity-mediated inhibition of *Crithidia mellificae* and *Lotmaria passim* growth by *Lactobacillus* spent media. Growth rates of *C. mellificae* (upper panels) and *L. passim* (lower panels) in spent media (A, C) of *Lactobacillus melliventris* strains wkB8 (left) and wkB10 (center) before and after neutralization from pH 4.6 to 5.6 with 1M NaOH, and in fresh *Lactobacillus* media (right) with and without acidification from pH 5.6 to 4.6 with acetic acid. Boxplots show medians and interquartile range for n = 6 samples per group. Points show individual observations, horizontally offset to mitigate overplotting.

Temperature-dependent effects of *Lactobacillus* on *Lotmaria passim* growth in parasite-symbiont cocultures. In parasite-symbiont cocultures, the presence of *Lactobacillus* altered the thermal niche of *L. passim* by inhibiting the parasite's growth in a temperature-dependent fashion **(Figure 4).** The 95% confidence intervals for model-predicted parasite growth rates in the presence and absence of *Lactobacillus* overlapped below 23 °C, but the symbiont's presence had increasingly pronounced inhibitory effects as temperature increased **(Figure 4).** These effects resulted in a 24% lower predicted peak parasite growth rate and a 1.9 °C reduction in the temperature at which parasite growth declined to less than 50% of peak rate, from 34.68 °C in the absence of *Lactobacillus* (95% CI: 34.16-35.55 °C) to 32.76 °C in its presence (95% CI: 32.06-33.46 °C) **(Figure 5)**. Confidence intervals for other parameters and traits overlapped in the two *Lactobacillus* treatments **(Supplementary Figures 3 and 4).**

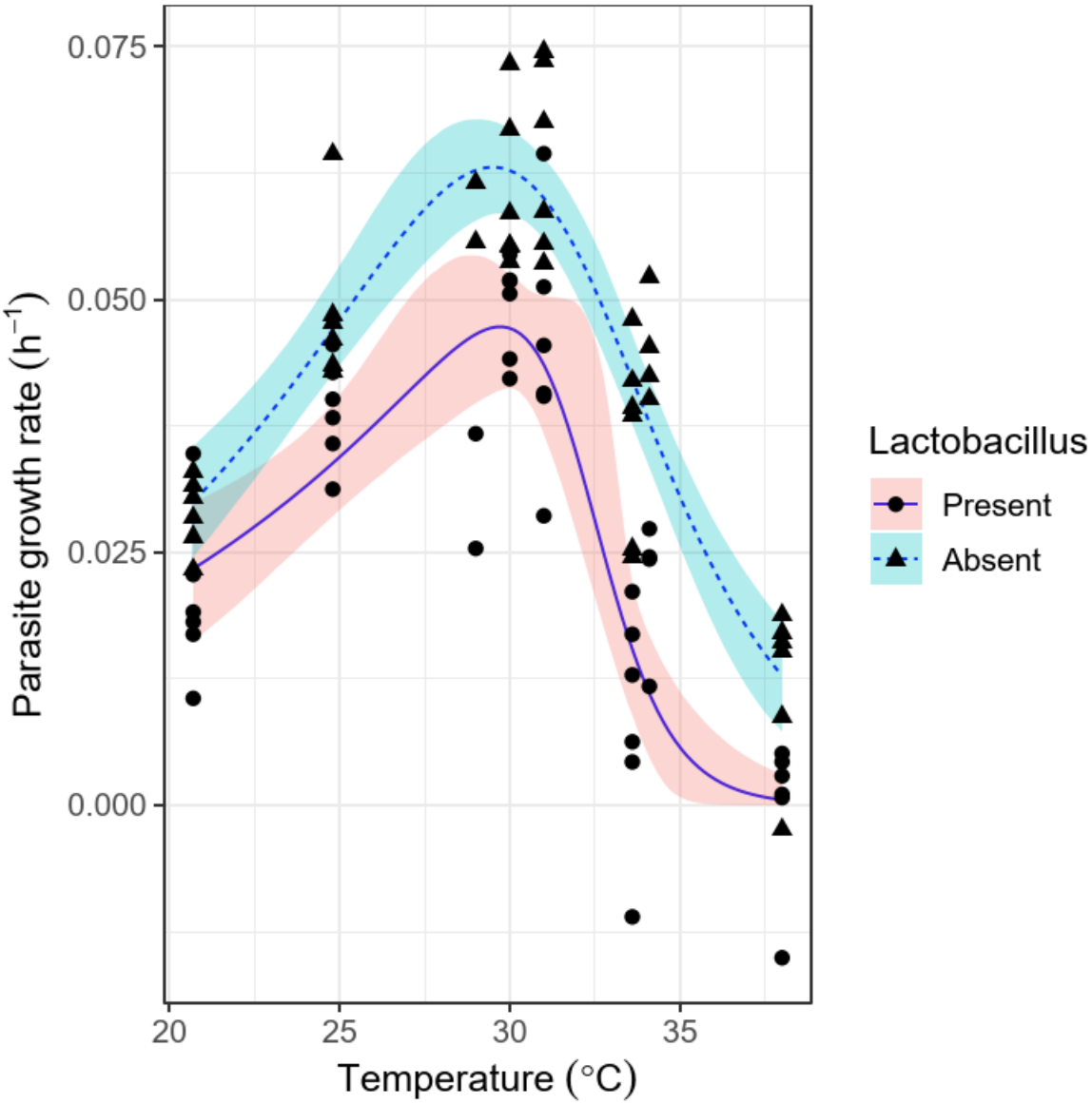

285

286 **Figure 4. Coculture with *Lactobacillus* affects *Lotmaria passim* growth in a temperature-dependent**

287 **manner,** with stronger effects of the symbiont at higher temperatures. Lines and shaded bands show

288 Sharpe-Schoolfield model fits and 95% confidence intervals for *L. passim* growth rate in the presence

289 (solid lines) and absence (dashed lines) of *Lactobacillus*. Points show individual observations; circles and

290 triangles indicate presence and absence of *Lactobacillus,* respectively.

291

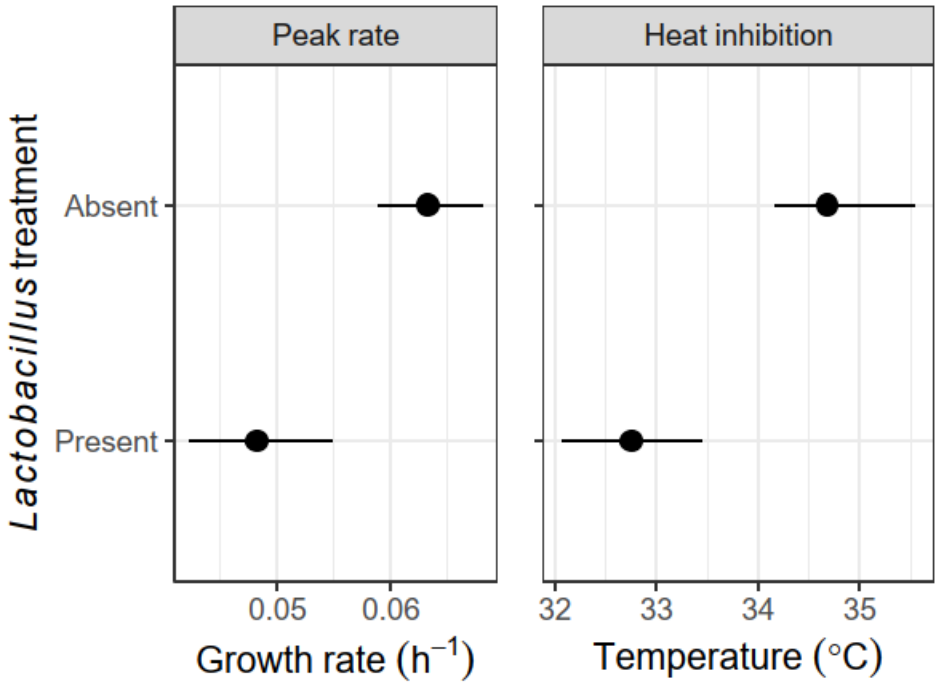

Figure 5. The presence of *Lactobacillus* reduced peak *Lotmaria passim* growth rate (left) and lowered the temperature at which growth rate declined to <50% of peak value (right). Points and error bars show estimates and 95% bootstrap confidence intervals for traits derived from Sharpe-Schoolfield model fits shown in Figure 4.

The inhibitory effects of *Lactobacillus* increased quadratically with temperature (Temperature: coefficient -25.71 ± 8.82 SE, Z = -2.91, P = 0.004; Temperature^2: coefficient 0.51 ± 0.15 SE, Z = 3.39, P < 0.001); inhibition exceeded 50% at 32.9 °C (95% CI: 30.26-34.82 °C, **Figure 6A**). The final pH of the coculture decreased by 0.098 ± 0.0060 SE pH units per 1 °C increase in temperature (Z = -16.38, P < 0.001, **Figure 6B**). Across all temperatures, stronger inhibitory effects of *Lactobacillus* were quadratically correlated with lower final pH (pH: coefficient -707.75 ± 203.32 SE, Z = -3.48, P < 0.001; pH^2: coefficient 65.60 ± 20.05 SE, Z = 3.27, P = 0.001), with 50% reduction in growth at a final pH of 4.69 (95% CI: 4.52-4.96, **Figure 6C**).

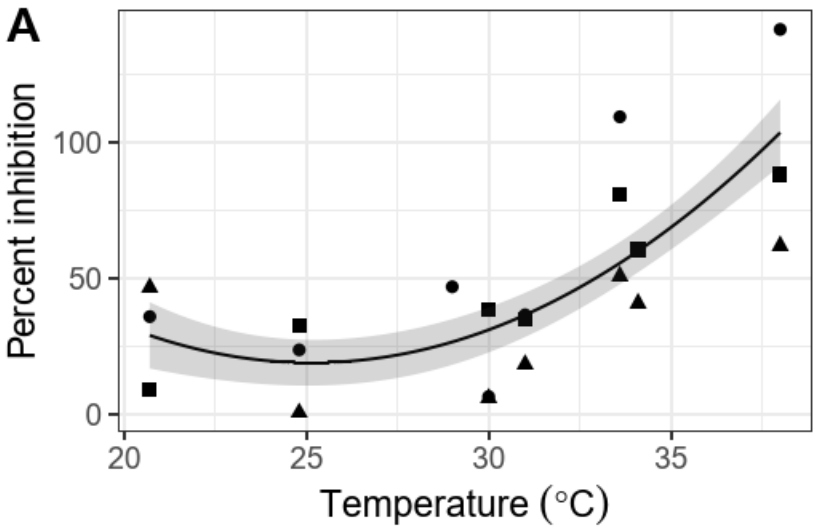

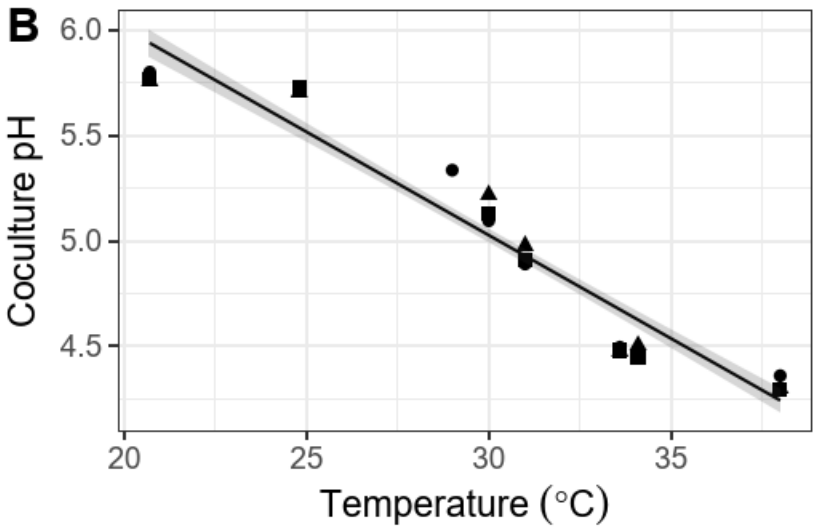

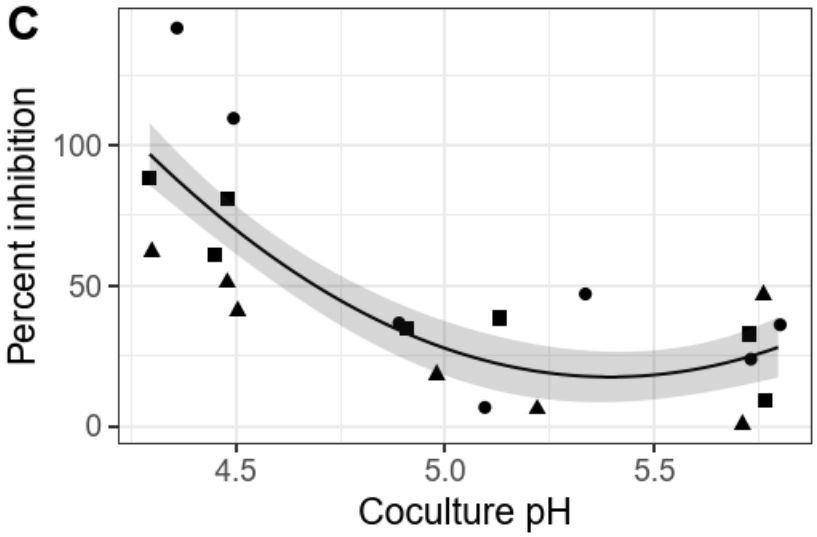

306

Figure 6. Temperature-dependent, pH-associated effects of *Lactobacillus* on growth of *Lotmaria passim* in symbiont-parasite cocultures. (A) Proportional inhibitory effects of *Lactobacillus* on *L. passim* increased with temperature**. (B**) Higher temperatures resulted in lower pH of the growth media**. (C**) Lower pH was correlated with greater proportional inhibition of *L. passim* growth. Lines and shaded bands show estimated marginal means and standard errors of linear model predictions. Points show individual observations. Shapes indicate different experimental blocks.

DISCUSSION

Due to the fundamental effects of temperature on biological rates, including parasite and symbiont growth and metabolism, temperature has the potential to alter the effects of symbionts on parasite establishment, such that both symbiont and parasite physiology shape the temperature dependence of infection. We found that high temperatures augmented growth rates of symbionts relative to parasites, that symbionts inhibited parasite growth via production of acids, and that high temperatures amplified this inhibitory effect.

Symbionts were more heat-tolerant than parasites. Our finding of greater heat tolerance in the honey bee symbiont than in the trypanosomatids is consistent with differences in conventional culturing temperatures and results from bumble and honey bee-associated microbes. Most trypanosomatids are cultured at 25-28 °C (63), whereas honey bee gut bacteria thrive at 35-37 °C (22). The ~6 °C lower peak growth temperature of *L. passim* relative to the *Lactobacillus* symbionts closely resembles the difference in peak temperatures for *C. bombi* (~34 °C) and *Lactobacillus bombicola* (~40 °C) from bumble bees (44). Other key symbionts of honey bees are also heat-tolerant and able to grow above 40 °C (64). In our experiments, the *Lactobacillus* symbiont's greater heat tolerance and temperature responsiveness led to rapid changes in the relative growth rates of symbionts vs. parasites, especially the less heat-tolerant *L.*

passim, over the temperature range found in colony-dwelling honey bees (20-37 °C (21)). This suggests that honey bees' endothermic behavior could select for growth of coevolved symbionts at the expense of opportunistic parasites. Although both trypanosomatids were still able to grow above 34 °C, growth rates of *Lactobacillus* relative to the parasites (especially *L. passim*) increased particularly sharply over the 33.8-37 °C range of the colony's core during the brood-rearing season (20). This indicates that the warm temperatures at the center of the colony would favor formation of a core symbiont-dominated microbiome during the microbiome's formative period in the 2-4 days after emergence of adults from pupation, including primacy of *Lactobacillus* Firm-5 species in the rectum (41).

Symbiont-produced acids inhibited parasite growth. Although growth rates depicted suitability of the colony habitat for trypanosomatids relative to symbionts, growth of symbionts is only directly relevant to proliferation of parasites if there is some interaction between the two. We found that *Lactobacillus*-spent medium inhibited growth of both honey bee parasites in an acidity-dependent manner within the gut pH range observed in bees. Environmental pH is a strong driver of gut microbiome composition (65), where single-unit changes in pH alter the relative growth rates of cooccurring species and community-level production of short-chain fatty acids (66). Production of acids by fermentative bacteria, including Lactobacilli, contributes strongly to their chemical inhibition of gut parasites (67, 68). In humans, diets that acidify stool pH from 6.5 to 5.5 are associated with suppression of opportunistically pathogenic Enterobacteriaceae species, such as *E. coli*, that grow poorly in acidic environments (69). Similarly, supplementation of infants with milk sugar-fermenting *Bifidobacteria* reduces stool pH from 5.97 to 5.15 and reduces levels of Enterobacteriaceae, Clostridiaceae, and endotoxins (70), whereas reduced levels of Bifidobacteria have been associated with a 1.5-unit increase in fecal pH and increased abundance of Enterobacteriaceae, Clostridiaceae, and other dysbiosis-associated bacteria over the past century (71).

In the gut of honey bees, one effect of bacterial colonization is a nearly identical reduction in hindgut pH, from pH ~6 to pH ~5.2 (57). A major contributor to this acidification is likely the *Lactobacillus* Firm-5 species cluster, which alone was responsible for around 90% of the chemical changes seen in the gut metabolome of honey bees with intact microbial communities (43). Our findings of *Lactobacillus* acidity-mediated inhibition of honey bee trypanosomatids are consistent with pH-dependent inhibition of *C. bombi* by *Lactobacillus bombicola* from bumble bees (45), and match the negative correlations between *C. bombi* infection intensity and abundances of acid-producing *Lactobacillus* and *Gilliamella* in these hosts (38, 40). Our results also show a strong correlation between pH and *L. passim* growth in cocultures, with inhibition occurring over a physiologically relevant range. The rectal pH of adult bees in colonies ranged between 4.2 and 6.0 (72). Whereas pre-colonization of bees with *Snodgrassella alvi*—which consumes organic acids (43)—increased *L. passim* infection (48), we found that an endpoint coculture pH below 5 was associated with sharply reduced *L. passim* growth rates, suggesting that microbial or climatic factors that acidify gut pH to the lower end of this observed range would improve resistance to infection. Such acidity-driven pressure on parasites could be one explanation for honey bee parasites' high tolerance of acidity relative to trypanosomatids from insects with less acidic guts (51).

High temperatures amplified the parasite-inhibiting effects of symbionts. Our coculture experiments showed that the inhibitory effects of symbionts on parasites increased with temperature. Both *Lactobacillus* strains grew faster and produced acids more rapidly as temperatures increased over the range found in bee colonies. This high-temperature inhibition resulted in lower peak parasite growth rates and reduced parasite heat tolerance relative to when symbionts were absent. Hence, social bees' endothermic maintenance of high colony temperatures could exert antiparasitic effects not only through direct parasite inhibition, but also via potentiation of the parasite-inhibiting effects of symbionts. The bumble bee symbiont *Lactobacillus bombicola* resulted in similar temperature-

dependent inhibition of the parasite *C. bombi,* lowering the temperature of peak parasite growth rate and resulting in a more rapid decline in parasite growth rate as temperatures increased (44). Using a parasite-symbiont system from a related host, our results build on these findings by investigating a broader range and increased number of temperatures, enabling formal comparisons between parasite thermal performance curves in the presence vs. absence of symbionts.

The manipulability of both microbiome and body temperature in a host with a predominantly endothermic life history strategy makes honey bees a useful system to explore the value of endothermy as a reinforcer of symbioses and symbiont-mediated defense against parasites. Prior work has shown that high (35 °C) temperatures increase resistance of honey bees to colonization by heat-sensitive environmental yeasts relative to cooler (29 °C) temperatures, consistent with the seasonal appearance of yeasts during colder weather in field-collected forager bees (73). On the other hand, high (35 °C) temperatures enhanced growth of and gut colonization by the core symbiont *S. alvi* in bumble bees relative to low (28-29 °) temperatures (64). These results implicate bee endothermy in both resistance to opportunistic gut microbes and establishment of key symbionts.

Our results indicate that higher temperatures not only promote symbiont growth, but also augment symbionts' value as a defense against gut parasites. Consistent with this idea, honey bees collected from cooler winter colonies exhibit gut colonization by non-core microbial taxa in addition to—rather than in place of—their pre-existing core symbionts (42), suggesting that the core symbiont community's resistance to invasion requires high temperatures even when its major members, including *Lactobacillus* Firm-5, are abundant (42). Temperature-mediated inhibition of trypanosomatids specifically is of practical importance for honey bees, where infection intensities were highest mid-winter in one longitudinal survey (36) and correlated with winter colony collapse in another (26).

399 Environmental factors that perturb thermoregulation, such as exposure to pesticides, agricultural
400 landscapes, and food shortage (21, 74–76), could exacerbate this seasonal susceptibility.

401

402 CONCLUSIONS

403 The presence of parasites can shift the thermal niche of hosts towards temperatures that
404 enhance escape from or suppression of infection (15). High body temperatures often mitigate infection
405 of warm-adapted hosts, including honey bees and other insects (10, 77–80), with less heat-adapted
406 parasites (8). Conversely, the host's responses to temperature can alter the optimal temperature for
407 parasite reproduction (5, 8). Our findings complement these results, showing how the presence of gut
408 symbionts can limit both peak growth rate and heat tolerance of a globally prevalent honey bee gut
409 parasite. The extent of symbiont-mediated inhibition varied substantially over the range of
410 temperatures and gut pH levels previously reported in adult bees, indicating the potential for
411 endothermic behavior and core gut symbionts of honey bees to synergistically inhibit parasite growth.
412 Our finding that high temperatures promote symbiont-mediated parasite inhibition shows how changes
413 in host temperature could augment or diminish the protective effects of the microbiome against
414 infection. This illustrates an interaction between the well-established effects of temperature and gut
415 microbial communities on resistance to parasites, with implications for understanding the effects of
416 climate on infection of ectotherms and the evolution of endothermy and fever. The ability of symbionts
417 to shift the thermal niche of parasites highlights the value of investigating parasite thermotolerance in
418 the context of the host microbiota.

419

ACKNOWLEDGMENTS

We thank the ATCC, R.S. Schwarz, J.E. Powell, and N.J. Moran for microbial strains and culturing advice; Daniel Padfield for R scripts; and anonymous reviewers for their service in improving the manuscript.

FUNDING

This project was supported by USDA-NIFA Postdoctoral Fellowship 2022-67012-37482 to ECPY; USDA-NIFA Pollinator Health Grant 2020-67013-31861 to JDE and ECPY; a North American Pollinator Protection Campaign Honey Bee Health Improvement Project Grant and an Eva Crane Trust Grant to ECPY and JDE, and the USDA Agricultural Research Service Beltsville Bee Research Laboratory in house fund. Funders had no role in study design, data collection and interpretation, or publication. We thank the reviewers for their service in improving the manuscript.

CONFLICTS OF INTEREST

The authors declare that they have no conflicts of interest.

DATA AVAILABILITY

All data are supplied in the Supplementary Information, Data S1.

AUTHORS' CONTRIBUTIONS

ECPY conceived the study. ECPY and LM designed experiments. ECPY, LM, and WFH conducted experiments. ECPY analyzed data. ECPY and LM drafted the manuscript with guidance from JDE. All authors revised the manuscript and gave approval for publication.

REFERENCES

1. Brown JH, Gillooly JF, Allen AP, Savage VM, West GB. 2004. Toward a Metabolic Theory of Ecology. Ecology 85:1771–1789.

2. Gillooly JF, Brown JH, West GB, Savage VM, Charnov EL. 2001. Effects of Size and Temperature on Metabolic Rate. Science 293:2248–2251.

3. Dell AI, Pawar S, Savage VM. 2014. Temperature dependence of trophic interactions are driven by asymmetry of species responses and foraging strategy. J Anim Ecol 83:70–84.

4. Dell AI, Pawar S, Savage VM. 2011. Systematic variation in the temperature dependence of physiological and ecological traits. Proc Natl Acad Sci 108:10591–10596.

5. Kirk D, Jones N, Peacock S, Phillips J, Molnár PK, Krkošek M, Luijckx P. 2018. Empirical evidence that metabolic theory describes the temperature dependency of within-host parasite dynamics. PLOS Biol 16:e2004608.

6. Raffel TR, Romansic JM, Halstead NT, McMahon TA, Venesky MD, Rohr JR. 2013. Disease and thermal acclimation in a more variable and unpredictable climate. Nat Clim Change 3:146–151.

7. Molnár PK, Sckrabulis JP, Altman KA, Raffel TR. 2017. Thermal Performance Curves and the Metabolic Theory of Ecology—A Practical Guide to Models and Experiments for Parasitologists. J Parasitol 103:423–439.

8. Cohen JM, Venesky MD, Sauer EL, Civitello DJ, McMahon TA, Roznik EA, Rohr JR. 2017. The thermal mismatch hypothesis explains host susceptibility to an emerging infectious disease. Ecol Lett 20:184–193.

9. Blanford S, Thomas MB. 1999. Host thermal biology: the key to understanding host–pathogen interactions and microbial pest control? Agric For Entomol 1:195–202.

10. Thomas MB, Blanford S. 2003. Thermal biology in insect-parasite interactions. Trends Ecol Evol 18:344–350.

11. Stahlschmidt ZR, Adamo SA. 2013. Context dependency and generality of fever in insects. Naturwissenschaften 100:691–696.

12. Kluger MJ, Kozak W, Conn CA, Leon LR, Soszynski D. 1998. Role of Fever in Disease. Ann N Y Acad Sci 856:224–233.

13. Hollings M. 1965. Disease control through virus-free stock. Annu Rev Phytopathol 3:367–396.

14. Cevallos RC, Sarnow P. 2010. Temperature Protects Insect Cells from Infection by Cricket Paralysis Virus. J Virol 84:1652–1655.

15. Padfield D, Castledine M, Buckling A. 2020. Temperature-dependent changes to host–parasite interactions alter the thermal performance of a bacterial host. 2. ISME J 14:389–398.

16. Boltaña S, Rey S, Roher N, Vargas R, Huerta M, Huntingford FA, Goetz FW, Moore J, Garcia-Valtanen P, Estepa A, MacKenzie S. 2013. Behavioural fever is a synergic signal amplifying the innate immune response. Proc R Soc B 280:20131381.

17. Casadevall A. 2016. Thermal Restriction as an Antimicrobial Function of Fever. PLoS Pathog 12:e1005577.

18. Spor A, Koren O, Ley R. 2011. Unravelling the effects of the environment and host genotype on the gut microbiome. Nat Rev Microbiol 9:279–290.

19. Sepulveda J, Moeller AH. 2020. The Effects of Temperature on Animal Gut Microbiomes. Front Microbiol 11.

20. Fahrenholz L, Lamprecht I, Schricker B. 1989. Thermal investigations of a honey bee colony: thermoregulation of the hive during summer and winter and heat production of members of different bee castes. J Comp Physiol B 159:551–560.

21. Esch H. 1960. Über die Körpertemperaturen und den Wärmehaushalt von *Apis mellifica*. Z Für Vgl Physiol 43:305–335.

22. Engel P, James RR, Koga R, Kwong WK, McFrederick QS, Moran NA. 2013. Standard methods for research on *Apis mellifera* gut symbionts. J Apic Res 52:1–24.

23. Romero S, Nastasa A, Chapman A, Kwong WK, Foster LJ. 2019. The honey bee gut microbiota: strategies for study and characterization. Insect Mol Biol 28:455–472.

24. Raymann K, Moran NA. 2018. The role of the gut microbiome in health and disease of adult honey bee workers. Curr Opin Insect Sci 26:97–104.

25. Evans JD, Schwarz RS. 2011. Bees brought to their knees: microbes affecting honey bee health. Trends Microbiol 19:614–620.

26. Cornman RS, Tarpy DR, Chen Y, Jeffreys L, Lopez D, Pettis JS, vanEngelsdorp D, Evans JD. 2012. Pathogen Webs in Collapsing Honey Bee Colonies. PLOS ONE 7:e43562.

27. Higes M, Martín-Hernández R, Garrido-Bailón E, González-Porto AV, García-Palencia P, Meana A, del Nozal MJ, Mayo R, Bernal JL. 2009. Honeybee colony collapse due to *Nosema ceranae* in professional apiaries. Environ Microbiol Rep 1:110–113.

499 28. Langridge DF, McGhee RB. 1967. *Crithidia mellificae* n. sp. an acidophilic trypanosomatid of the
500 honey bee *Apis mellifera*. J Protozool 14:485–487.

501 29. Schwarz RS, Bauchan GR, Murphy CA, Ravoet J, de Graaf DC, Evans JD. 2015. Characterization of
502 Two Species of Trypanosomatidae from the Honey Bee *Apis mellifera*: *Crithidia mellificae*
503 Langridge and McGhee, and *Lotmaria passim* n. gen., n. sp. J Eukaryot Microbiol 62:567–583.

504 30. Liu Q, Lei J, Darby AC, Kadowaki T. 2020. Trypanosomatid parasite dynamically changes the
505 transcriptome during infection and modifies honey bee physiology. 1. Commun Biol 3:1–8.

506 31. Gómez-Moracho T, Buendía-Abad M, Benito M, García-Palencia P, Barrios L, Bartolomé C, Maside
507 X, Meana A, Dolores Jiménez-Antón M, Isabel Olías-Molero A, María Alunda J, Martín-Hernández
508 R, Higes M. 2020. Experimental evidence of harmful effects of Crithidia mellificae and Lotmaria
509 passim on honey bees. Int J Parasitol 50:1117–1124.

510 32. Vejnovic B, Stevanovic J, Schwarz RS, Aleksic N, Mirilovic M, Jovanovic NM, Stanimirovic Z. 2018.
511 Quantitative PCR assessment of Lotmaria passim in Apis mellifera colonies co-infected naturally
512 with Nosema ceranae. J Invertebr Pathol 151:76–81.

513 33. Arismendi N, Bruna A, Zapata N, Vargas M. 2016. PCR-specific detection of recently described
514 Lotmaria passim (Trypanosomatidae) in Chilean apiaries. J Invertebr Pathol 134:1–5.

515 34. Morimoto T, Kojima Y, Yoshiyama M, Kimura K, Yang B, Peng G, Kadowaki T. 2013. Molecular
516 detection of protozoan parasites infecting Apis mellifera colonies in Japan. Environ Microbiol Rep
517 5:74–77.

35. Waters TL. 2018. The distribution and population dynamics of the honey bee pathogens Crithidia mellificae and Lotmaria passim in New Zealand. Te Herenga Waka-Vic Univ Wellingt Thesis https://doi.org/10.26686/wgtn.17068349.v1.

36. Runckel C, Flenniken ML, Engel JC, Ruby JG, Ganem D, Andino R, DeRisi JL. 2011. Temporal analysis of the honey bee microbiome reveals four novel viruses and seasonal prevalence of known viruses, *Nosema* , and *Crithidia*. PLOS ONE 6:e20656.

37. Koch H, Schmid-Hempel P. 2011. Socially transmitted gut microbiota protect bumble bees against an intestinal parasite. Proc Natl Acad Sci U S A 108:19288–19292.

38. Koch H, Schmid-Hempel P. 2012. Gut microbiota instead of host genotype drive the specificity in the interaction of a natural host-parasite system. Ecol Lett 15:1095–1103.

39. Kwong WK, Medina LA, Koch H, Sing K-W, Soh EJY, Ascher JS, Jaffé R, Moran NA. 2017. Dynamic microbiome evolution in social bees. Sci Adv 3:e1600513.

40. Mockler BK, Kwong WK, Moran NA, Koch H. 2018. Microbiome Structure Influences Infection by the Parasite Crithidia bombi in Bumble Bees. Appl Environ Microbiol 84:e02335-17.

41. Powell JE, Martinson VG, Urban-Mead K, Moran NA. 2014. Routes of Acquisition of the Gut Microbiota of the Honey Bee Apis mellifera. Appl Environ Microbiol 80:7378–7387.

42. Kešnerová L, Emery O, Troilo M, Liberti J, Erkosar B, Engel P. 2020. Gut microbiota structure differs between honeybees in winter and summer. 3. ISME J 14:801–814.

43. Kešnerová L, Mars RAT, Ellegaard KM, Troilo M, Sauer U, Engel P. 2017. Disentangling metabolic functions of bacteria in the honey bee gut. PLOS Biol 15:e2003467.

538 44. Palmer-Young EC, Raffel TR, McFrederick Quinn S. 2018. Temperature-mediated inhibition of a
539 bumblebee parasite by an intestinal symbiont. Proc R Soc B Biol Sci 285:20182041.

540 45. Palmer-Young EC, Raffel TR, McFrederick QS. 2019. pH-mediated inhibition of a bumble bee
541 parasite by an intestinal symbiont. Parasitology 146:380–388.

542 46. Palmer-Young EC, Ngor L, Nevarez RB, Rothman JA, Raffel TR, McFrederick QS. 2019. Temperature
543 dependence of parasitic infection and gut bacterial communities in bumble bees. Environ
544 Microbiol 21:4706–4723.

545 47. Louradour I, Monteiro CC, Inbar E, Ghosh K, Merkhofer R, Lawyer P, Paun A, Smelkinson M,
546 Secundino N, Lewis M, Erram D, Zurek L, Sacks D. 2017. The midgut microbiota plays an essential
547 role in sand fly vector competence for *Leishmania major*. Cell Microbiol 19:e12755.

548 48. Schwarz RS, Moran NA, Evans JD. 2016. Early gut colonizers shape parasite susceptibility and
549 microbiota composition in honey bee workers. Proc Natl Acad Sci 113:9345–9350.

550 49. Kwong WK, Mancenido AL, Moran NA. 2014. Genome Sequences of Lactobacillus sp. Strains wkB8
551 and wkB10, Members of the Firm-5 Clade, from Honey Bee Guts. Genome Announc 2:e01176-14.

552 50. Salathé R, Tognazzo M, Schmid-Hempel R, Schmid-Hempel P. 2012. Probing mixed-genotype
553 infections I: Extraction and cloning of infections from hosts of the trypanosomatid *Crithidia bombi*.
554 PLOS ONE 7:e49046.

555 51. Palmer-Young EC, Raffel TR, Evans JD. 2021. Hot and sour: parasite adaptations to honeybee body
556 temperature and pH. Proc R Soc B 288:20211517.

557 52. Padfield D, Yvon-Durocher G, Buckling A, Jennings S, Yvon-Durocher G. 2016. Rapid evolution of
558 metabolic traits explains thermal adaptation in phytoplankton. Ecol Lett 19:133–142.

559 53. Schoolfield RM, Sharpe PJH, Magnuson CE. 1981. Non-linear regression of biological temperature-
560 dependent rate models based on absolute reaction-rate theory. J Theor Biol 88:719–731.

561 54. Padfield D, O'Sullivan H, Pawar S. 2021. rTPC and nls.multstart: A new pipeline to fit thermal
562 performance curves in r. Methods Ecol Evol 12:1138–1143.

563 55. Fox J, Weisberg S. 2011. An R companion to applied regressionSecond Ed. Sage, Thousand Oaks CA.
564 http://socserv.socsci.mcmaster.ca/jfox/Books/Companion.

565 56. R Core Team. 2014. R: A language and environment for statistical computing. R Foundation for
566 Statistical Computing, Vienna, Austria. http://www.R-project.org.

567 57. Zheng H, Powell JE, Steele MI, Dietrich C, Moran NA. 2017. Honeybee gut microbiota promotes
568 host weight gain via bacterial metabolism and hormonal signaling. Proc Natl Acad Sci 114:4775–
569 4780.

570 58. Palmer-Young EC, Schwarz RS, Chen Y, Evans JD. 2022. Punch in the gut: Parasite tolerance of
571 phytochemicals reflects host diet. Environ Microbiol 24:1805–1817.

572 59. Brooks ME, Kristensen K, Benthem KJ van, Magnusson A, Berg CW, Nielsen A, Skaug HJ, Maechler
573 M, Bolker BM. 2017. glmmTMB Balances Speed and Flexibility Among Packages for Zero-inflated
574 Generalized Linear Mixed Modeling. R J 9:378–400.

575 60. Lenth R. 2019. emmeans: Estimated Marginal Means, aka Least-Squares Means. https://CRAN.R-
576 project.org/package=emmeans.

577 61. Wickham H. 2009. ggplot2: elegant graphics for data analysis. Springer New York.
578 http://had.co.nz/ggplot2/book.

579 62. Wilke CO. 2016. cowplot: streamlined plot theme and plot annotations for “ggplot2.” CRAN Repos
580 https://CRAN.R-project.org/package=cowplot.

581 63. Schmittner SM, McGhee RB. 1970. Host Specificity of Various Species of Crithidia Léger. J Parasitol
582 56:684–693.

583 64. Hammer TJ, Le E, Moran NA. 2021. Thermal niches of specialized gut symbionts: the case of social
584 bees. Proc R Soc B Biol Sci 288:20201480.

585 65. Ilhan ZE, Marcus AK, Kang D-W, Rittmann BE, Krajmalnik-Brown R. 2017. pH-Mediated Microbial
586 and Metabolic Interactions in Fecal Enrichment Cultures. mSphere 2:e0047-17.

587 66. Walker AW, Duncan SH, McWilliam Leitch EC, Child MW, Flint HJ. 2005. pH and peptide supply can
588 radically alter bacterial populations and short-chain fatty acid ratios within microbial communities
589 from the human colon. Appl Environ Microbiol 71:3692–3700.

590 67. Gorbach SL. 1990. Lactic Acid Bacteria and Human Health. Ann Med 22:37–41.

591 68. Adams MR, Hall CJ. 1988. Growth inhibition of food-borne pathogens by lactic and acetic acids and
592 their mixtures. Int J Food Sci Technol 23:287–292.

593 69. Zimmer J, Lange B, Frick J-S, Sauer H, Zimmermann K, Schwiertz A, Rusch K, Klosterhalfen S, Enck P.
594 2012. A vegan or vegetarian diet substantially alters the human colonic faecal microbiota. Eur J Clin
595 Nutr 66:53–60.

596 70. Frese SA, Hutton AA, Contreras LN, Shaw CA, Palumbo MC, Casaburi G, Xu G, Davis JCC, Lebrilla CB,
597 Henrick BM, Freeman SL, Barile D, German JB, Mills DA, Smilowitz JT, Underwood MA. 2017.
598 Persistence of Supplemented Bifidobacterium longum subsp. infantis EVC001 in Breastfed Infants.
599 mSphere 2:e00501-17.

71. Henrick BM, Hutton AA, Palumbo MC, Casaburi G, Mitchell RD, Underwood MA, Smilowitz JT, Frese SA. 2018. Elevated Fecal pH Indicates a Profound Change in the Breastfed Infant Gut Microbiome Due to Reduction of Bifidobacterium over the Past Century. mSphere 3.

72. Rademacher E, Harz M, Schneider S. 2017. Effects of Oxalic Acid on Apis mellifera (Hymenoptera: Apidae). 3. Insects 8:84.

73. Kogan HV, Elikan AB, Glaser KF, Bergmann JM, Raymond LM, Prado-Irwin SR, Snow JW. 2023. Colonization of Honey Bee Digestive Tracts by Environmental Yeast Lachancea thermotolerans Is Naturally Occurring, Temperature Dependent, and Impacts the Microbiome of Newly Emerged Bees. Microbiol Spectr 0:e05194-22.

74. Meikle WG, Weiss M, Maes PW, Fitz W, Snyder LA, Sheehan T, Mott BM, Anderson KE. 2017. Internal hive temperature as a means of monitoring honey bee colony health in a migratory beekeeping operation before and during winter. Apidologie 48:666–680.

75. Tosi S, Démares FJ, Nicolson SW, Medrzycki P, Pirk CWW, Human H. 2016. Effects of a neonicotinoid pesticide on thermoregulation of African honey bees (Apis mellifera scutellata). J Insect Physiol 93–94:56–63.

76. Heinrich B. 1972. Patterns of endothermy in bumblebee queens, drones and workers. J Comp Physiol 77:65–79.

77. Martín-Hernández R, Meana A, García-Palencia P, Marín P, Botías C, Garrido-Bailón E, Barrios L, Higes M. 2009. Effect of temperature on the biotic potential of honeybee microsporidia. Appl Environ Microbiol 75:2554–2557.

620 78. James RR. 2005. Temperature and chalkbrood development in the alfalfa leafcutting bee,
621 Megachile rotundata. Apidologie 36:15–23.

622 79. Starks PT, Blackie CA, Seeley TD. 2000. Fever in honeybee colonies. Naturwissenschaften 87:229–
623 231.

624 80. Dalmon A, Peruzzi M, Le Conte Y, Alaux C, Pioz M. 2019. Temperature-driven changes in viral loads
625 in the honey bee Apis mellifera. J Invertebr Pathol 160:87–94.

626

Supplementary information

SUPPLEMENTARY FIGURES

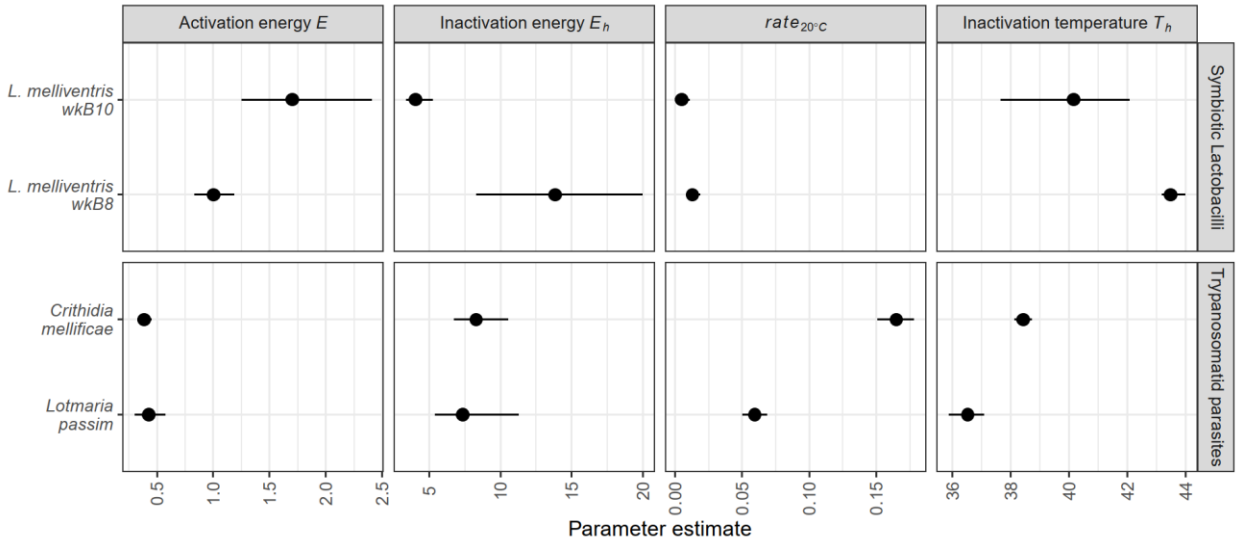

Supplementary Figure 1. Model parameter estimates for Sharpe-Schoolfield models. Parameters *E* and E_h (measured in eV) indicate how strongly growth rate responds to temperature below and above the temperature of peak growth, respectively. The growth rate at 20 °C (measured in h^{-1}) indicates the speed of growth at a reference temperature at which no high-temperature inhibition of growth is expected. Parameter T_h (calculated in K, shown in °C) indicates the temperature at which growth rate is inhibited by 50% relative to the rate predicted by the upward-sloping (Arrhenius) portion of the thermal performance curve, which assumes a monotonic increase of growth rate with increasing temperature. Points and error bars show bootstrap medians and 95% confidence intervals.

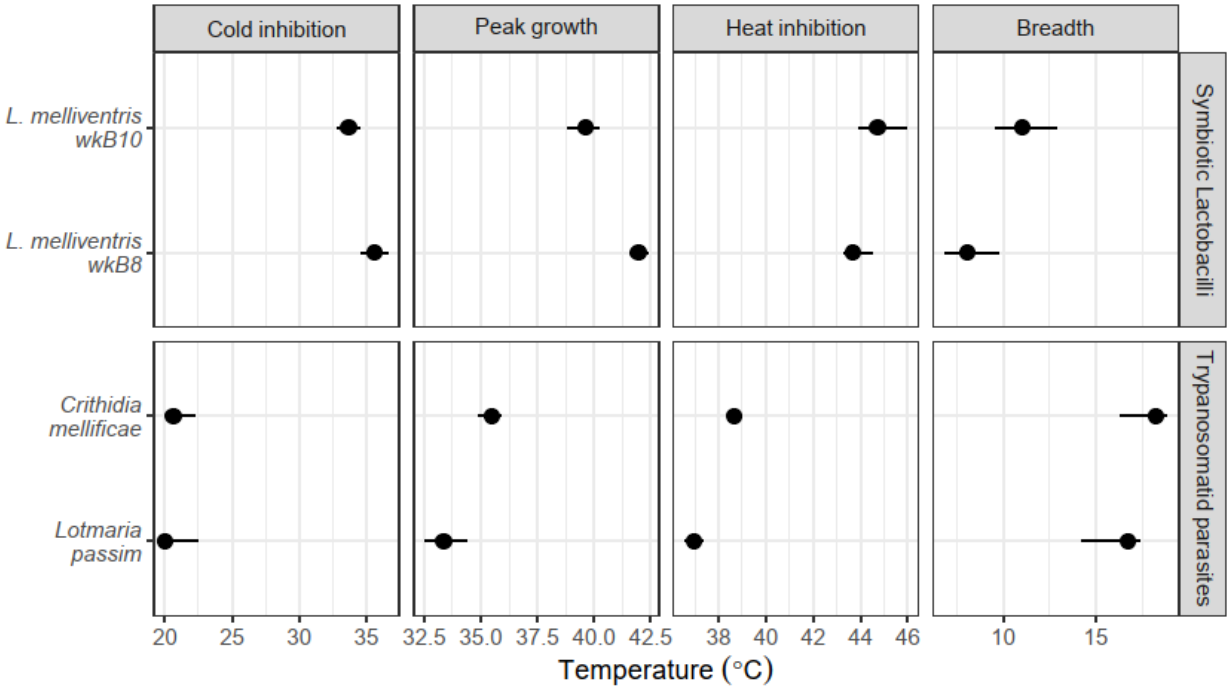

641

642

643 **Supplementary Figure 2. Estimates of derived quantities from Sharpe-Schoolfield models** for

644 temperatures of peak growth, 50% inhibition due to cold and hot temperatures, and thermal niche

645 breadth. Panel for "Peak growth" shows the temperature at which peak growth rate occurs. Panels for

646 "Cold inhibition" and "Heat inhibition" show the temperatures at which growth is reduced by 50%

647 relative to the peak growth rate. "Breadth" indicates the size of the temperature interval over which

648 growth rate is at least half of maximum, calculated as the difference between the temperatures of cold

649 and heat inhibition. Points and error bars show bootstrap medians and 95% confidence intervals.

650

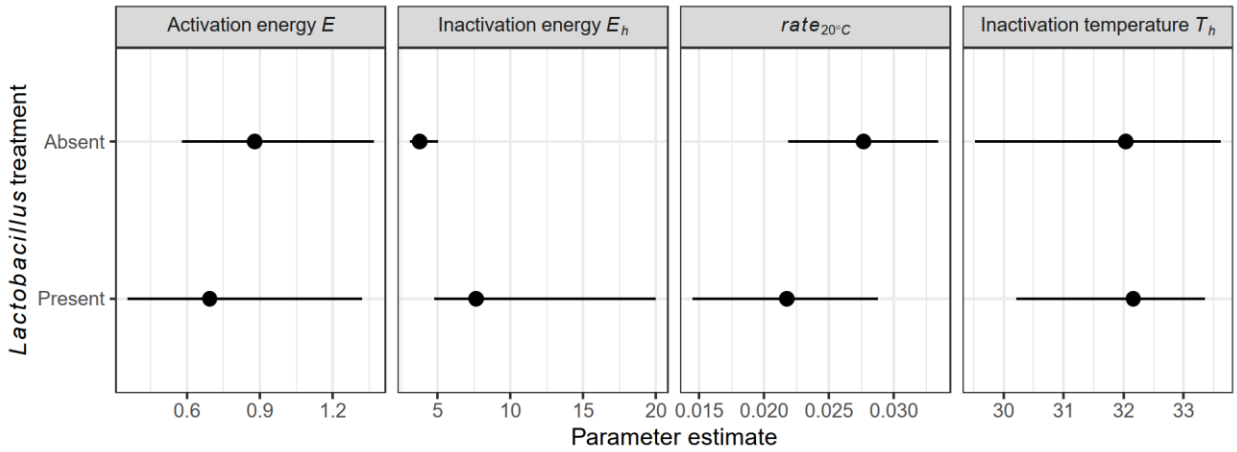

651

652 **Supplementary Figure 3. Model parameter estimates for Sharpe-Schoolfield models** for *Lotmaria*
653 *passim* growth in the presence and absence of *Lactobacillus*. Parameters E and E_h (measured in eV)
654 indicate how strongly growth rate responds to temperature below and above the temperature of peak
655 growth, respectively. The growth rate at 20 °C (measured in h^{-1}) indicates the speed of growth at a
656 reference temperature at which no high-temperature inhibition of growth is expected. Parameter T_h
657 (calculated in K, shown in °C) indicates the temperature at which growth rate is inhibited by 50% relative
658 to the rate predicted by the upward-sloping (Arrhenius) portion of the thermal performance curve,
659 which assumes a monotonic increase of growth rate with increasing temperature. Points and error bars
660 show bootstrap medians and 95% confidence intervals.

661

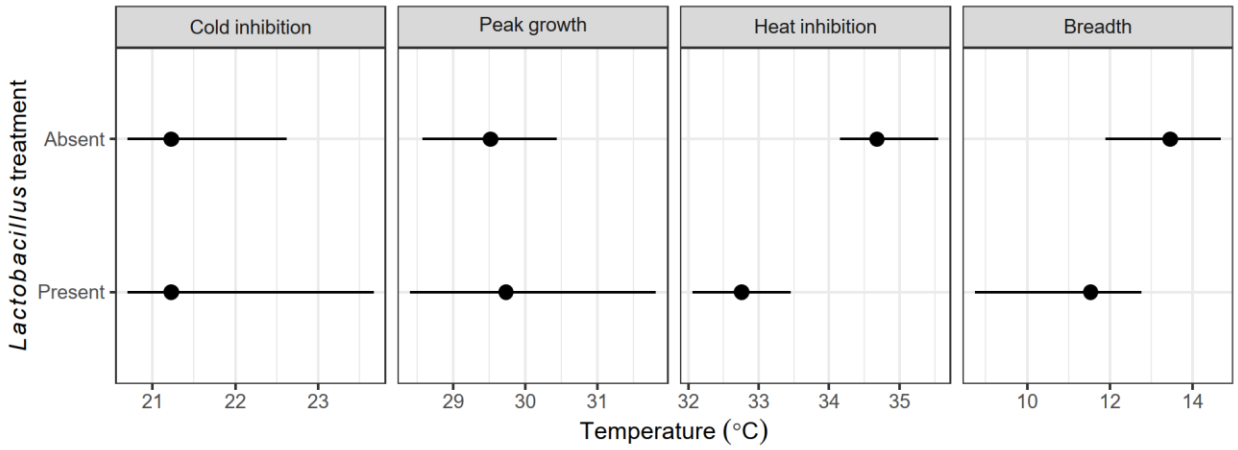

662

663 **Supplementary Figure 4. Estimates of derived quantities from Sharpe-Schoolfield models** of *L. passim*

664 growth in the presence and absence of *Lactobacillus.* Panels for "Cold inhibition" and "Heat inhibition"

665 show the temperatures at which growth is reduced by 50% relative to the peak growth rate. "Breadth"

666 indicates the size of the temperature interval over which growth rate is at least half of maximum,

667 calculated as the difference between the temperatures of cold and heat inhibition. Points and error

668 bars show bootstrap medians and 95% confidence intervals.

669

670

671

672

673

674

675

SUPPLEMENTARY DATA

Supplementary Data S1 (.zip). Zipped file containing raw data with separate text files for growth rates of *Lactobacillus* and trypanosomatids in isolation; growth of trypanosomatids with *Lactobacillus* spent medium; growth of *L. passim* in cocultures; and summaries of Sharpe-Schoolfield models for *Lactobacillus* and trypanosomatids in isolation and *L. passim* -*Lactobacillus* cocultures.